Quantum Chemistry Study of Actinide(III) and Lanthanide(III) Complexes with Tridentate Nitrogen Ligands

Dominique Guillaumont*

Commissariat à l'Energie Atomique, Valrhô, DEN/DRCP/SCPS/LCAM, Bât. 166, BP 17171, 30207 Bagnols-sur-Cèze, France

Received: April 2, 2004; In Final Form: June 8, 2004

The structure and bonding in large complexes of actinide(III) and lanthanide(III) with tridentate N-donor ligands and water molecules have been investigated through quantum chemistry calculations in order to characterize the nature of the lanthanide−ligand and actinide−ligand bonds. Calculations have been performed using relativistic density functional theory on $[M(L)(H_2O)_6]^{3+}$, $[M(L)(H_2O)_5Cl]^{2+}$, and $[M(H_2O)_9]^{3+}$ clusters where M = La, Ce, Nd, U, Pu, Am, or Cm and L = 2,2′:6′2″terpyridine (Terpy) or 2,6-bis(5,6-dimethyl-1,2,4-triazin-3-yl)pyridine (MeBtp). Calculated M−L distances compare well with X-ray crystal data obtained on related systems. In particular, calculations correctly reproduce the experimentally observed shortening of the uranium−ligand bond in comparison with the cerium−ligand bond. The calculated evolution of the M−L bond as a function of the cation shows that lanthanide−ligand distances decrease with the diminution of the ionic radius, whereas the actinide−ligand distances increase from uranium to americium and are shorter than Ln−N distances. These trends are explained by the presence of slightly stronger covalent effects in the metal−ligand bond for the actinides, decreasing in the order U > Pu > Am ≈ Cm, compared to lanthanides. The participation of 5f orbitals in the bonding is found to be significant only for uranium.

1. Introduction

The separation of trivalent minor actinides (americium(III), curium(III)) from trivalent lanthanides in the wastes produced by nuclear fuel reprocessing is an active field of investigation.[1] Actinide and lanthanide cations in the trivalent oxidation state have very similar chemical properties in aqueous solution; they are both strongly hydrated and present similar ionic radii.[2,3] Finding ligands able to separate them through liquid/liquid solvent extraction processes is a particularly difficult task. Hard Lewis bases form purely ionic complexes and cannot achieve the separation. On the other hand, softer Lewis bases are expected to form bonds with a slightly greater covalent character with actinides than with lanthanides.[4] This subtle electronic effect is attributed to the ability of valence orbitals of actinides, especially 5f, to participate in bonding, whereas 4f orbitals of lanthanides are lower in energy and less spatially expanded and are often considered as core orbitals. This electronic effect is expected to be small but has been exploited to design some families of soft donor ligands, and successful separations have been obtained through liquid/liquid extraction processes. Among soft donor ligands, tridentate N-donor aromatic bases, such as 2,4,6-tri(pyridin-2-yl)-1,3,5-triazine (Tptz), 2-amino-4,6-di(pyridin-2-yl)-1,3,5-triazine (Adptz), 2,6-bis(5,6-di-alkyl-1,2,4-triazin-3-yl)pyridine (RBtp), and 2,2′:6′2″-terpyridine (Terpy), have shown a good ability to separate americium(III) from lanthanide(III) and are some of the most extensively investigated ligands.[5−10] Separation factors over 100 from nitric acid solution into an organic phase have been obtained with RBtp ligands.[9] However, although several tridentate N-donor ligands give rise to high separation factors, some other ligands of the same family present very poor separation properties.[7,8]

Understanding the mechanism of ligand binding to metal cation is essential for finding ligands that demonstrate enhanced effectiveness. Considerable progress has been made in this area.[11−14] In particular, the nature of the metal−ligand bond has been probed through thermodynamic studies and crystal structure determinations in order to characterize the differences between actinide and lanthanide ligand bonds. X-ray structures of complexes formed between uranium(III), cerium(III) and Terpy, Pr^{n}Btp ligands have been determined by Berthet et al.[14] and Iveson et al.;[13] they show that the mean U−N(ligand) bond lengths are from 0.05 to 0.09 Å shorter than the corresponding Ce−N distances, even though the ionic radii of Ce^{3+} and U^{3+} are very similar. Recently, thermodynamic studies related to the extraction of europium(III) and americium(III) by a Pr^{n}Btp ligand have shown that the enthalpy term is the driving force for the extraction of both metal ions and for the americium(III)/europium(III) selectivity. The enthalpy variation between the trivalent cations is small ($\Delta(\Delta H°)_{Am/Eu} = -11$ kJ·mol^{-1} in octan-1-ol and $NaNO_3$) but suggests slightly stronger Am−N bonds than Eu−N bonds.[15] Moreover, the thermodynamics of the complexation of trivalent lanthanides and actinides with Adptz in aqueous solution has been the subject of a very recent systematic study.[16] The comparison of the thermodynamic parameters of the two series of f-elements shows that the enthalpy term is a few kJ·mol^{-1} more negative for actinide complexes, resulting in increased stability of the complexes by a factor of 20 in favor of the actinide cations. Computational studies on the model complexes $[M(pyrazine)_3I_3]$ (M = La, Nd, U) point to the shortening of the M−N(pyrazine) bond from lanthanum to uranium because of the presence of π-back-donation from the 5f orbitals of uranium into the π^* orbitals of the pyrazine.[17] Overall, these recent basic studies on tridentate nitrogen aromatic ligands with actinide(III) and lanthanide(III) support the idea of stronger actinide−nitrogen bonds with some

* E-mail: dominique.guillaumont@cea.fr.

10.1021/jp048550x CCC: $27.50
Published on Web 07/28/2004

SCHEME 1

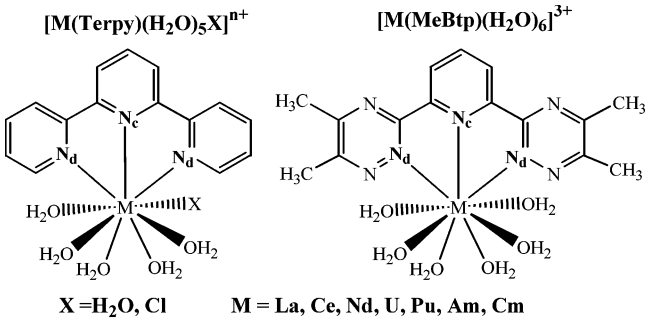

covalent character. However, no structural data are available for americium(III) and curium(III), and no thermodynamic parameters have been measured for uranium(III) because of the experimental difficulties in obtaining X-ray spectra for radioactive Am or Cm and in stabilizing the trivalent U in solution. Even though uranium(III) is generally considered as an actinide analogue of americium(III) and curium(III), the metal−ligand bond may be different across the actinide series.

We report here the results of a systematic quantum chemistry study of actinide(III) and lanthanide(IIII) complexes with tridentate N-donor aromatic ligands in order to characterize and compare the evolution of the metal−ligand bond within a series of trivalent cations from a structural and electronic standpoint. Actinide compounds remain a challenge for quantum chemistry and the study was motivated in large part by the rare opportunity to confront quantum chemistry results on actinide(III) with the experimental work recently done on the systems of interest.

Calculations have been carried out on $[M(L)(H_2O)_6]^{3+}$, $[M(L)(H_2O)_5Cl]^{2+}$, and $[M(H_2O)_9]^{3+}$ clusters where M is a trivalent cation belonging to the first half of the lanthanides (lanthanum, cerium, neodymium) or actinides (uranium, plutonium, americium, curium) series (Scheme 1). The lanthanide cations were selected because their ionic radii are comparable with the actinides of interest. Two tridentate ligands were chosen for the study, Terpy and MeBtp. MeBtp was taken as a model for the RBtp ligands. The choice of the ligands was motivated by the available experimental data; in particular, X-ray structures with lanthanide(III) and uranium(III) would provide a test of the calculated structures. The choice of the coordination sphere besides the ligand in the calculated structures was more intricate because of the various inner coordination spheres that have been reported in crystal structures of lanthanide(III) and uranium(III) complexes with Terpy or Btp ligands. A 9-coordinated structure with a neutral coordination sphere was first chosen considering that it is representative of a large number of experimental structures. Then, a few calculations on some of the complexes were done by replacing a water molecule with a chloride ion. Additionally, hydrated $[M(H_2O)_9]^{3+}$ clusters were calculated in order to compare M−O(H_2O) and M−N(ligand) bonds.

In the present investigation, the calculated metal−ligand bond distances computed at different calculations levels are compared. The calculated values are then compared with the available X-ray data to validate the theoretical approach for these large complexes of heavy elements. Finally the evolution of the metal−ligand bond within the series of cations is discussed.

2. Computational Details

2.1. Computational Methods. The calculations were performed using density functional theory (DFT) methods. Relativistic effects were considered by two different approaches, by the zeroth-order regular approximation (ZORA)[18−20] and through the use of relativistic effective core potentials (RECP).[21,22] Spin−orbit effects were not taken into account. Several studies have shown that these two DFT methods reproduce the experimental geometries of lanthanide and actinide compounds with satisfactory accuracy.[23−29] For open-shell systems, unrestricted DFT methods were employed.

The DFT/ZORA calculations were performed using the Amsterdam Density Functional (ADF) program package.[30−32] Uncontracted triple-ζ Slater-type valence orbitals with one set of polarization functions were used for all atoms. The frozen-core approximation was used where the core density was obtained from four-component Dirac−Slater calculations on all of the atoms and kept frozen during molecular calculations. $1s^2$ core electrons were frozen for carbon, nitrogen, and oxygen and $(1s2s2p)^{10}$ for chlorine. The valence space of the heavy elements includes 5s, 5p, 5d, 4f, 6s shells of lanthanides and 6s, 6p, 6d, 5f, 7s shells of actinides. The numerical integration parameter in ADF was set to 6.0. The density functional consists of a local density part using the parametrization of Vosko, Wilk, and Nusair and exchange-correlation gradient corrected parts of Becke[33] and Perdew[34] (BVP86).

RECP-based calculations were performed with the Gaussian 98 package.[35] Energy-adjusted RECPs developed in the Stuttgart and Dresden groups were used together with the accompanying basis set to describe the valence electron density.[21,22] Small-core RECPs replace 60 core electrons for actinides and 28 electrons for the lanthanides, whereas large-core RECPs for lanthanides put 5s, 5p, 6d, and 6s shells in the valence space. The corresponding valence basis sets associated with small-core pseudopotentials are 14s13p10d8f basis contracted to 10s8p5d4f for lanthanides and 12s11p9d8f contracted to 8s7p6d4f for actinides. The basis set associated with lanthanides large-core pseudopotentials is 7s6p5d contracted to 5s4p3d. On other atoms the 6-31G* basis was employed. The BP86[33,34] functional as well as the hybrid B3LYP functional[36,37] were employed. The use of DFT with a 6-31G* basis set was tested through preliminary calculations. They were done on small $[M(H_2O)]^{3+}$ and $[M(Py)]^{3+}$ systems, where M = La, Pm, Gd, Lu, U, Cm and Py = pyridine using 6-31G, 6-31G*, 6-31+G*, and 6-311+G(2d,p) basis set at the DFT(B3LYP) and MP2 levels. The difference between the metal−ligand bond distances (M−O(H_2O), M−N(Py)) calculated at the MP2 and DFT level is $\leq$0.02 Å. Increasing the size of the basis set from 6-31G* to 6-31+G* and 6-311+G(2d,p) basis set at the DFT level led to small decreases of about 0.01 Å of the metal−ligand bond length.

The structures of the complexes were fully optimized without symmetry constraint. The initial conformations of the complexes were deduced from crystallographic data, and vibrational frequencies were calculated analytically for $[La(Terpy)(H_2O)_6]^{3+}$, $[La(MeBtp)(H_2O)_6]^{3+}$, $[Cm(Terpy)(H_2O)_6]^{3+}$, and $[Cm(MeBtp)(H_2O)_6]^{3+}$ to ensure that the optimized structures are true minima (with no imaginary frequencies).

All complexes except La(III) systems are open shell with a $4f^n$ ground-state configuration for lanthanide(III) and a $5f^n$ configuration for actinide(III); $n = 1$ for Ce, $n = 3$ for Nd and U, $n = 5$ for Pu, $n = 6$ for Am, and $n = 7$ for Cm. This results in several low-lying electronic states with different f electron occupations and spin states. To determine the electronic ground-state configuration, all possible spin states of $[M(Terpy)(H_2O)_6]^{3+}$ complexes were calculated with ADF. For all Terpy complexes, the calculations give the highest spin state as the ground state. Therefore, considering the similar nature of Terpy,

TABLE 1: Electronic Ground-State Configuration of Ln(III) and An(III) Complexes (C_1 Symmetry)

metal ion	4f occupation	ground state	metal ion	5f occupation	ground state
La	$4f^0$	^1A	U	$5f^3$	^4A
Ce	$4f^1$	^2A	Pu	$5f^5$	^6A
Nd	$4f^3$	^4A	Am	$5f^6$	^7A
			Cm	$5f^7$	^8A

TABLE 2: Calculated M−N and M−O Bond Distances (Å) in Terpy and MeBtp Complexes of Lanthanum and Curium at Different Levels of Approximations

cluster	method	M−N_c	M−N_d	<M−O>[a]
$[La(Terpy)(H_2O)_6]^{3+}$	LC/BP86	2.660	2.646	2.662
	SC/B3LYP	2.638	2.620	2.658
	SC/BP86	2.632	2.609	2.649
	ZORA/BVP86	2.632	2.618	2.658
$[Cm(Terpy)(H_2O)_6]^{3+}$	SC/B3LYP	2.553	2.560	2.587
	SC/BP86	2.539	2.547	2.575
	ZORA/BVP86	2.535	2.545	2.592
$[La(MeBtp)(H_2O)_6]^{3+}$	SC/BP86	2.709	2.687	2.606
	ZORA/BVP86	2.702	2.674	2.599
$[Cm(MeBtp)(H_2O)_6]^{3+}$	SC/BP86	2.605	2.595	2.523
	ZORA/BVP86	2.595	2.593	2.533

[a] Average of the six M−O(H_2O) distances.

MeBtp, and aqua complexes, the results reported in the next sections were obtained from ground-state configurations with the highest spin multiplicity (indicated in Table 1).

Solvent effects were estimated for one of the complex ($[La(Terpy)(H_2O)_6]^{3+}$) through the polarizable continuum model using the polarizable conductor calculation model.[38] The solute cavity was built using UATM radii.[39]

2.2. Comparison of Calculated Metal−Ligand Distances at Different Levels of Theory. The complexes under consideration were initially calculated using relativistic effective core potentials at the DFT level. Eventually, because of the difficulty of obtaining the SCF convergence with RECPs for actinides with an open 5f shell other than $5f^7$, we did not use this approach for all the complexes. Because the ADF implementation allowed the convergence of these systems, the ZORA approach was finally chosen. In this part, we compare the calculated structural parameters of lanthanum and curium complexes that have been successfully calculated with the two approaches. RECP calculations were performed employing large- and small-core (LC, SC) RECPs for Ln and small-core (SC) for An at the DFT level using two different functionals. Table 2 compares the computed metal-to-ligand and metal-to-water interatomic distances at the different levels of calculations. Other structural parameters are not reported here since our main interest is in the comparison of the metal−ligand bonds.

Very good agreement was found between RECP (SC) and ZORA results. The maximum difference between the optimized bond distances is 0.02 Å and corresponds to the curium−oxygen distance. Lanthanum−nitrogen and curium−nitrogen bond distances agree within 0.01 Å between the two approaches. However, the very good agreement found between the two approaches for La and Cm cannot be extrapolated to other actinide elements that may have more covalent metal−ligand bonds. In particular, a recent DFT study on $M(L)I_3$ complexes with M = La, Nd, U and L = $NCCH_3$, CO showed that the RECP approach in conjunction with a hybrid functional gives much longer U−N($NCCH_3$) and U−C(CO) bond distances than the ZORA approach with a GGA functional.[40]

It is noteworthy that the RECPs results show a significant decrease in the bond distances when going from small-core to large-core RECPs (up to 0.03 Å) for the lanthanum complex. Metal−ligand bond distances obtained with B3LYP and BP86 density functionals are very close; BP86 values are only about 0.01 Å shorter than B3LYP values.

3. Results and Discussion

3.1. Comparison of Calculated with Observed Structures. A large number of crystal structures of lanthanide(III) ions with tridentate N-donor aromatic ligands have been resolved in various experimental conditions. For a given cation and ligand, depending on the solution (solvent and counterions), rare earth complexes crystallize into different structures with various inner coordination spheres. In the presence of weakly coordinating counterions and solvent, 1:3 complexes $[M(L)_3]^{3+}$ are routinely obtained, whereas in strongly coordinating environment such as water with nitrate or chloride ions, 1:1 and 1:2 complexes are observed with an inner coordination sphere that includes solvent molecules and counterions. The coordination number (CN) and the nature of the species present in the first coordination sphere in addition to the nitrogen ligand(s) have a significant effect on the metal−nitrogen bond distances. Variations of a 0.1 Å in the distances are routinely observed in the crystal structures. In contrast, actinide(III) structures are very scarce, and to our knowledge, only uranium(III) structures have been resolved with nitrogen aromatic ligands. The few available uranium(III) crystal structures have been obtained under the same experimental conditions as for some cerium(III) structures, so they are analogous complexes and can be directly compared.

Terpy Systems. From the Cambridge Structural Database[41,42] we retrieved respectively 12, 6, and 7 crystal structures of lanthanum(III), cerium(III), and neodymium(III) complexes with terpyridine. The structures correspond to 1:1, 1:2, and 1:3 complexes; the coordination numbers range from 9 to 11 for lanthanum(III), from 8 to 11 for cerium(III), and from 8 to 10 for neodymium(III). Metal−nitrogen(Terpy) bond distances vary from 2.63 to 2.79 Å for La, from 2.60 to 2.71 Å for Ce, and from 2.58 to 2.70 Å for Nd. Table 3 shows the bond distances between the cation and the coordinating nitrogen atom for the most relevant calculated and experimental structures. Crystal structures of $[Ln(Terpy)(H_2O)_5Cl]^{2+}$ structures have been resolved for the Ln series,[43] whereas the $[Ln(Terpy)(H_2O)_6]^{3+}$ structure has been crystallized only for lanthanum. Therefore, calculated $[Ln(Terpy)(H_2O)_6]^{3+}$ structures are compared with $[Ln(Terpy)_3]^{3+}$ crystal structures with the same coordination number and with a neutral coordination sphere. We assume that steric effects between Terpy ligands in $[Ln(Terpy)_3]^{3+}$ (Ln = Ce, Nd) are small enough not to alter Ln−N distances as observed in $[La(Terpy)(H_2O)_6]^{3+}$ and $[La(Terpy)_3]^{3+}$ crystal structures that present very similar mean La−N distances.

Calculated and experimental M−N distances in $[Ln(Terpy)(H_2O)_5Cl]^{2+}$ (Ln = La, Ce, Nd) agree within 0.01−0.04 Å. When no counterion is present in the first coordination sphere, calculated metal−ligand bond distances become shorter as a result of the increased charge on the cluster and the absence of solvent beyond the first coordination sphere in the model structures. Thus, calculated Ln−N distances in $[Ln(Terpy)(H_2O)_6]^{3+}$ (Ln = La, Ce, Nd) are 0.05−0.07 Å shorter than experimental distances found in the analogous $[La(Terpy)(H_2O)_6]^{3+}$ and $[Ln(Terpy)_3]^{3+}$ clusters. Optimizing the geometry of $[La(Terpy)(H_2O)_6]^{3+}$ including solvent effects through a polarized continuum model increases the computed values of La−N distances and provides better agreement with experimental values (within 0.03 Å). The trends in M−N distances measured when going from La to Ce and Nd is correctly

TABLE 3: Calculated and Experimental M−N Bond Distances (Å) in Terpy and MeBtp Complexes

		$M-N_c$		$<M-N_d>$[c]	
calculated structure	crystal structure	calcd	expt	calcd	expt
$[La(Terpy)(H_2O)_5Cl]^{2+}$[a]	$[La(Terpy)(H_2O)_5Cl]^{2+}$ (ref 43)	2.67	2.688(4)	2.65	2.658(3)
$[Ce(Terpy)(H_2O)_5Cl]^{2+}$[a]	$[Ce(Terpy)(H_2O)_5Cl]^{2+}$ (ref 43)	2.63	2.658(5)	2.62	2.643(4)
$[Nd(Terpy)(H_2O)_5Cl]^{2+}$[a]	$[Nd(Terpy)(H_2O)_5Cl]^{2+}$ (ref 43)	2.59	2.622(4)	2.57	2.613(3)
$[La(Terpy)(H_2O)_6]^{3+}$[a]	$[La(Terpy)(H_2O)_6]^{3+}$ (ref 55)	2.63	2.684(6)	2.62	2.66(1)
$[La(Terpy)(H_2O)_6]^{3+}$ sol.[b]		2.68		2.63	
$[La(Terpy)(H_2O)_6]^{3+}$[a]	$[La(Terpy)_3]^{3+}$ (ref 56)	2.63	2.686(4)	2.62	2.67(4)
$[Ce(Terpy)(H_2O)_6]^{3+}$[a]	$[Ce(Terpy)_3]^{3+}$ (ref 56)	2.59	2.662(7)	2.58	2.64(4)
$[Nd(Terpy)(H_2O)_6]^{3+}$[a]	$[Nd(Terpy)_3]^{3+}$ (ref 56)	2.58	2.63(1)	2.57	2.63(4)
$[U(Terpy)(H_2O)_6]^{3+}$[a]	$[U(Terpy)_3]^{3+}$ (ref 56)	2.52	2.623(2)	2.53	2.63(4)
$[La(MeBtp)(H_2O)_6]^{3+}$[a]	$[La\ (MeBtp)_3]^{3+}$ (ref 56)	2.70	2.67(2)	2.67	2.63(2)
$[Ce(MeBtp)(H_2O)_6]^{3+}$[a]	$[Ce(MeBtp)_3]^{3+}$ (ref 55)	2.65	2.64(2)	2.62	2.61(2)
	$[Ce(Pr^nBtp)_3]^{3+}$ (ref 55)		2.64(1)		2.60(4)
$[U(MeBtp)(H_2O)_6]^{3+}$[a]	$[U(Pr^nBtp)_3]^{3+}$ (ref 55)	2.56	2.55(2)	2.54	2.54(2)

[a] ZORA/BVP86 calculations. [b] Calculated using a continuum solvent approach and RECP(SC)/BP86. [c] Average of the two $M-N_d$ distances.

TABLE 4: Calculated Metal−Nitrogen and Metal−Oxygen Bond Distances (Å) in $[M(L)(H_2O)_6]^{3+}$ Complexes (ZORA/BVP86 Calculations)

	$[M(Terpy)(H_2O)_6]^{3+}$				$[M(MeBtp)(H_2O)_6]^{3+}$				$[M(H_2O)_6]^{3+}$
metal ion	$M-N_c$	$<M-N_d>$	$<M-O>$	Δd[a]	$M-N_c$	$<M-N_d>$	$<M-O>$	Δd[a]	$<M-O>$
La	2.632	2.618	2.658	+0.01	2.702	2.674	2.599	+0.07	2.611
Ce	2.589	2.584	2.630	+0.01	2.648	2.624	2.567	+0.05	2.579
Nd	2.579	2.570	2.599	+0.03	2.649	2.620	2.546	+0.08	2.547
U	2.517	2.527	2.624	−0.07	2.555	2.543	2.549	−0.04	2.589
Pu	2.538	2.556	2.618	−0.01	2.610	2.599	2.556	+0.04	2.560
Am	2.561	2.566	2.615	+0.01	2.624	2.611	2.555	+0.07	2.550
Cm	2.535	2.545	2.592	+0.00	2.595	2.593	2.533	+0.06	2.537

[a] Difference between the metal−oxygen distances in $[M(H_2O)_9]^{3+}$ and metal−nitrogen distances in $[ML(H_2O)_6]^{3+}$ (mean values).

reproduced by the calculations, in $[Ln(Terpy)(H_2O)_5Cl]^{2+}$ as well as in $[Ln(Terpy)(H_2O)_6]^{3+}$.

Crystal structures of uranium(III) with terpyridine correspond to 1:2 and 1:3 complexes (CN = 9) with triflate or iodide counterions in the first or second coordination sphere and with uranium−nitrogen distance varying from 2.59 to 2.68 Å. Calculated distances in $[U(Terpy)(H_2O)_6]^{3+}$ are 0.09−0.10 Å shorter than U−N distances in $[U(Terpy)_3]^{3+}$. Calculations underestimate U−N distances more than Ln−N distances. As a result, the M−N bond contraction observed experimentally from cerium to uranium is slightly overestimated by the calculations. The shortening of the mean M−N bond distance is 0.06 Å in $[M(Terpy)(H_2O)_6]^{3+}$ structures, whereas it is equal to 0.02 Å in $[M(Terpy)_3]^{3+}$ crystal structures and to 0.05 Å in $[M(Terpy)_2I_2]^{+}$ crystal structures.[14] Nevertheless, the agreement in the distances between experiment and calculation is satisfactory.

Btp Systems. Only a few crystal structures corresponding to complexes formed between lanthanides(III) and ligand belonging to the Btp family were retrieved from the Cambridge Structural Database. Five structures with neodymium(III) have been resolved with Btp substituted with ethyl, methyl, and isopropyl group and corresponding to 1:1, 1:2, and 1:3 complexes with a coordination number of nine or ten. Neodymium−nitrogen distances vary from 2.59 to 2.68 Å. For lanthanum(IIII), cerium(III), and uranium(III) only 1:3 complexes have been obtained with CN = 9 and no solvent molecule or counterion in the first coordination sphere. Three structures of 1:3 complexes of cerium(III) with MeBtp and EtBtp complexes have been resolved with Ce−N bond distances varying from 2.54 to 2.66 Å. A complex of lanthanum with MeBtp and uranium with Pr^nBtp has been crystallized; La−N distances range from 2.61 to 2.69 Å and U−N distances range from 2.52 to 2.59 Å.

For all of the cations, the calculations reproduce very well the experimental M−N distances observed in $[M(Btp)_3]^{3+}$ complexes. Computed Ce−N and U−N distances agree perfectly with X-ray measurements, whereas computed La−N distances are 0.03−0.04 Å longer than experimental values. The U−N/Ce−N bond contraction is also very well reproduced by the calculations: the $U-N_c$ bond length has been measured as 0.09 Å shorter than $Ce-N_c$ and the mean $U-N_d$ values as 0.08 Å shorter than the mean $Ce-N_d$ in $[M(Pr^nBtp)_3]^{3+}$; the calculated shortening in $[M(MeBtp)(H_2O)_6]^{3+}$ was 0.09 and 0.06 Å, respectively.

It is noteworthy that although the measured metal−nitrogen distances are shorter for MeBtp complexes than for Terpy complexes, calculations give the opposite trend and closer agreement with the experimental results for MeBtp than for Terpy complexes. A possible explanation is related to the nature of the metal−ligand bond. As discussed in the next section, the metal−ligand bond is slightly more covalent with MeBtp than with Terpy. Because of the limitation of the model systems with the absence of long-range solvent effects, a better description is expected for the metal−MeBtp bond than for the more electrostatic metal−Terpy bond for these charged complexes.

Aqua Cations. It is worth mentioning that the structures of trivalent lanthanides and a few actinide aqua complexes have been determined in aqueous solution with EXAFS, in the solid state with X-ray as well as through theoretical calculations. Our calculated values of metal-to-water distances in $[M(H_2O)_9]^{3+}$ clusters are indicated in the last column of Table 4. The plutonium(III)-to-water distances were measured in two EXAFS studies in dilute chloride solutions, with reported values of 2.49 and 2.51 Å (mean values),[44,45] and a crystal X-ray of $[Pu(H_2O)_9][CF_3SO_3]_3$ has been resolved[46] with a comparable distance of 2.51 Å. Previous theoretical calculations with ADF/ZORA on a $[Pu(H_2O)_9]^{3+}$ cluster predicted a value of 2.55 Å.[47] Our calculations, based on the same theoretical approach with a different density functional, give the very similar value of 2.56 Å. Water to trivalent americium, curium, lanthanum,

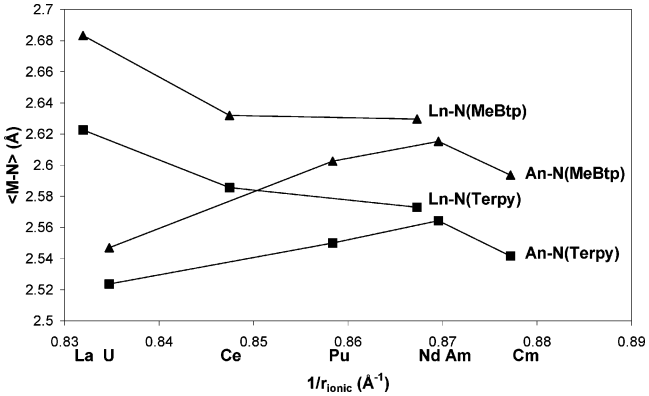

Figure 1. Evolution of M−N bond lengths versus the ionic radius of the trivalent metal in $[M(L)(H_2O)_6]^{3+}$.

cerium, and neodymium distances have been measured[45] by EXAFS under the same conditions as Pu, the reported values (in Å) were 2.49 (Am), 2.46 (Cm), 2.54 (La), 2.52 (Ce), and 2.49 (Nd) compared with our calculated values of 2.55 (Am), 2.54 (Cm), 2.61 (La), 2.58 (Ce), and 2.55 (Nd). For all of the cations, the calculated distances are 0.06−0.08 Å longer than measured values. The precise description of cation-to-water distances in $[M(H_2O)_n]^{q+}$ systems from quantum chemistry calculations is particularly difficult because of the strong cation−water interaction that remains effective beyond the first and even second solvation sphere, especially for highly charged +3 ions.[48−50] In the specific case of lanthanide ions, Cosentino et al.[39] have shown that the addition of a continuum representation of the solvent surrounding a $[Nd(H_2O)_9]^{3+}$ cluster leads to a decrease in the computed Nd−O distances of ∼0.04 Å and better agreement with the experimental findings. The systematic overestimation of the Ln−O and An−O distances in the present calculations performed on isolated clusters can be attributed in a large part to the absence of water molecules beyond the first coordination sphere. The relative evolutions of M−O distances in Ln and An series measured with EXAFS are reproduced by the calculation taking into account the experimental uncertainties of 0.01−0.02 Å in EXAFS distances.

3.2. Trends in the Metal−Ligand Bond. *Metal−Ligand Distances in* $[M(L)(H_2O)_6]^{3+}$. Table 4 gives the evolution of the metal−ligand bond distance calculated in $[M(H_2O)_9]^{3+}$, $[M(Terpy)(H_2O)_6]^{3+}$, and $[M(MeBtp)(H_2O)_6]^{3+}$ clusters. In the following, metal−nitrogen bond distances, metal−oxygen bond distances, and differences between the two will be discussed.

The trends in mean metal−nitrogen bond distances versus the reciprocal of the ionic radius of the metals are shown in Figure 1. A purely ionic bonding model would give a regular decrease of M−N distances with $1/r_{ionic}$. As can be seen from Figure 1 and Table 4, opposite trends are obtained for An−N and Ln−N bond distances. Although metal−nitrogen distances computed for the lanthanides follow the order La−N > Ce−N > Nd−N as expected from the diminishing ionic radius in the series, the calculated actinide−nitrogen distances increase at the beginning of the series in the order U−N < Pu−N < Am−N whereas the size of the ions increases in the series.The shortest M−N distances are obtained for uranium, which is the largest of the cations investigated here; for instance, U−N(MeBtp) distances are ∼0.07 Å shorter than for Cm−N(MeBtp), whereas the ionic radius of uranium(III) is 0.07 Å larger than that for curium(III). From Am to Cm, the An−N distances decrease with the diminishing ionic radii of the ions.

It is remarkable that An−N distances are all shorter than Ln−N distances for a given ligand and the considered metal ion. The smallest differences between An−N and Ln−N distances correspond to Am/Nd, which have a similar ionic radius.

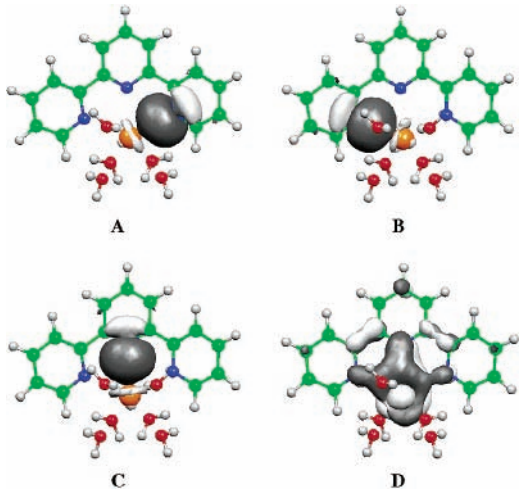

Figure 2. Localized molecular orbitals exhibiting covalency in metal−ligand bonds that are representative of the type present in the complexes: (A, B, C) ligand-to-metal σ-donation (σ_1, σ_2, σ_3); (D) metal-to-ligand π-back-donation (π_1). The orbitals shown correspond to $[U(Terpy)(H_2O)_6]^{3+}$.

Terpy and MeBtp ligands give rise to very similar trends in M−N bond distances. The main difference is the larger M−N diminution calculated from Pu to U for MeBtp than for Terpy.

In contrast, the trends in metal−oxygen distances calculated in $[ML(H_2O)_6]^{3+}$ and in $[M(H_2O)_9]^{3+}$ follow the expected decrease with the diminishing ionic radius of the metal cation. Thus, according to the ionic radius tabulated by Shannon[51] and David,[52,53] the size of the cations in the Ln series decreases by 0.02 Å from La to Ce and by 0.03 Å from Ce to Nd. In the An series, the differences in the ionic radii are 0.04 Å from U to Pu, 0.02 Å from Pu to Am, and 0.02 Å from Am to Cm. These values correspond to the calculated diminution of the metal−oxygen distances in the hydrated $[M(H_2O)_9]^{3+}$clusters (within ± 0.01 Å, see Table 4).

Table 4 indicates the difference Δd between the metal−oxygen distances in $[M(H_2O)_9]^{3+}$ and metal−nitrogen distances in $[ML(H_2O)_6]^{3+}$ (mean values). If we consider the complexation reaction by a tridentate ligand in water solution leading to the formation of a 1:1 complex, the reaction corresponds to the replacement of three water molecules bound to the metal by a ligand ($[M(H_2O)_9]^{3+} + L \rightarrow [ML(H_2O)_6]^{3+} + 3\ H_2O$). Δd is a useful parameter for qualitatively comparing the relative strength of M−N and M−O bond between the cations for a given ligand. Δd is positive and almost equal for the all the lanthanides cations, for Am and for Cm. Δd is slightly negative for Pu and significantly negative for U. Based on the Δd values, the strength of the metal-nitrogen bond relative to the metal−oxygen bond is comparable between the La, Ce, Nd, Am, and Cm, whereas it is slightly stronger for Pu and significantly stronger for U.

Electronic Structure of $[M(L)(H_2O)_6]^{3+}$ *Complexes*. The covalent bonding in these systems can be described in terms of a ligand-to-metal donation, involving the filled ligand σ and π molecular orbitals and the empty metal *n*s, $(n-1)$d, and $(n-2)$f orbitals (with $n = 7$ for An and $n = 6$ for Ln) and metal-to-ligand back-donation from the partially filled metal 4f or 5f orbitals to the empty ligand π^* molecular orbitals. This view of the bonding is supported by an analysis of the molecular orbitals involved in the metal−ligand bonding. According to the % contribution of the atomic orbitals to each molecular

TABLE 5: Percentage Contribution of Metal and Ligand Orbitals to Bonding M−L Molecular Orbitals (Boys−Foster Localized α-Spin Orbitals) in $[M(Terpy)(H_2O)_6]^{3+}$ and$[M(MeBtp)(H_2O)_6]^{3+}$[a]

	$[M(Terpy)(H_2O)_6]^{3+}$					$[M(MeBtp)(H_2O)_6]^{3+}$					
		M (%)			Terpy (%)		M (%)				MeBtp (%)
	description	d	f	s	total	description	d	f	s	p	total
La	σ_1(L→M)	6			91(σ)	σ_1(L→M)	5				94 (σ)
	σ_2(L→M)	6			91(σ)	σ_2(L→M)	5				93(σ)
	σ_3(L→M)	5			92(σ)	σ_3(L→M)	4				93(σ)
Ce	σ_1(L→M)	6			91(σ)	σ_1(L→M)	7				92(σ)
	σ_2(L→M)	6			91(σ)	σ_2(L→M)	5				93(σ)
	σ_3(L→M)	5			92(σ)	σ_3(L→M)	5				92(σ)
						π_1(M→L)		92			6(p*)
Nd	σ_1(L→M)	7			91(σ)	σ_1(L→M)	4				92 (σ)
	σ_2(L→M)	7			90(σ)	σ_2(L→M)	5	1			91(σ)
	σ_3(L→M)	5			91(σ)	σ_3(L→M)	5	1			92(σ)
U	σ_1(L→M)	7	1	1	91(σ)	σ_1(L→M)	6				91(σ)
	σ_2(L→M)	7	2	1	88(σ)	σ_2(L→M)	7	2	1		90(σ)
	σ_3(L→M)	7	2	1	90(σ)	σ_3(L→M)	6	1	1		91(σ)
	π_1(M→L)	2	76		16(π*)	π_1(M→L)		82	1	6	5(π*)
						π_2(M→L)	4	64			27(π*)
Pu	σ_1(L→M)	6	2	1	89(σ)	σ_1(L→M)	5		1		93(σ)
	σ_2(L→M)	6	3	1	90(σ)	σ_2(L→M)	5				94(σ)
	σ_3(L→M)	6	1	1	91(σ)	σ_3(L→M)	5	2	1		91(σ)
Am	σ_1(L→M)	6		1	92(σ)	σ_1(L→M)	6		1		92(σ)
	σ_2(L→M)	6		1	91(σ)	σ_2(L→M)	5		1		93(σ)
	σ_3(L→M)	6		1	90(σ)	σ_3(L→M)	5				94(σ)
Cm	σ_1(L→M)	6		1	91(σ)	σ_1(L→M)	6		1		94(σ)
	σ_2(L→M)	6		1	91(σ)	σ_2(L→M)	5		1		94(σ)
	σ_3(L→M)	6		1	92(σ)	σ_3(L→M)	5				93(σ)

[a] Only contributions greater or equal to 1% are reported. σ-type orbitals are doubly occupied whereas π-type orbitals are singly occupied.

TABLE 6: Calculated Mulliken and Hirshfeld Charges on the Metal Cation in $[M(Terpy)(H_2O)_6]^{3+}$, $[M(MeBtp)(H_2O)_6]^{3+}$, and $[M(H_2O)_9]^{3+}$ Clusters

	Terpy		MeBtp		H_2O	
metal ion	Mulliken	Hirshfeld	Mulliken	Hirshfeld	Mulliken	Hirshfeld
La	2.19	2.43	2.09	2.43	2.30	2.50
Ce	2.19	2.41	2.08	2.43	2.36	2.48
Nd	2.22	2.37	2.12	2.36	2.40	2.45
U	1.91	2.53	2.00	2.58	2.06	2.51
Pu	1.87	2.41	1.87	2.42	2.04	2.48
Am	1.80	2.39	1.85	2.44	2.00	2.48
Cm	1.82	2.43	1.84	2.44	1.99	2.50

orbital, only a few MOs show a mixing between the ligand and the metal orbitals. All molecular orbitals deriving from the ligand and the metal atomic orbitals and having a metal or ligand contribution at least greater or equal to 1% are listed in Table 5. For all metal centers, ligand-to-metal donation is found in three bonding molecular orbitals involving mainly the ligand σ orbital and the empty metal d orbitals (Figure 2A−C). The contributions (%) of the metals and ligand orbitals show that the molecular orbitals are mainly localized on the ligand. On the contrary, metal-to-ligand back-donation takes place mainly for uranium and to a lesser extent for Ce. For U, the donation involves a singly occupied 5f orbital and a π* with significant % contribution on the ligand, 16% on Terpy and 27% on MeBtp (Figure 2D). The most striking result is the absence of retro-donation from plutonium and americium. Except for U and Ce, the singly occupied 4f or 5f orbitals are pure with 99−100% 4f or 5f contribution.

The participation of empty s and f metal orbitals is greater for actinides than for lanthanides but remains weak for all of the cations. Overall, the total participation of the An center per σ bond is a few percent greater than the participation of Ln, for similarly size cations. However, the increase of charge transferred from the ligand to the metal when going from lanthanide to actinide is difficult to establish firmly. Although metal atomic charges determined from a Mulliken population analysis clearly show a diminution of the An charge in comparison with Ln denoting an increased charge transfer, a Hirshfeld decomposition scheme[54] give similar values for the actinide and lanthanide charges (Table 6). Mulliken charges are known to be strongly dependent on the atomic basis set and the large difference between An and Ln charges may be partly due to basis set differences between An and Ln. In the actinide series, Mulliken and Hirschfeld analysis give both the largest charge for U due to the metal-to-ligand back-donation.

To summarize, the metal−ligand bond is predominantly ionic. Covalency is present through ligand-to-metal electron donation and slightly more pronounced for actinides than for lanthanides although the differences reach the limits of the calculated approximations. Uranium is an exception with its ability to donate 5f electron to the ligand π* resulting in larger covalent effects in the U−N bond.

The larger contraction calculated for U−N(MeBtp) with respect to U−N(Terpy) distances in the actinides series is related to the larger 5f-π*(MeBtp) mixing than 5f-π*(Terpy). According to the calculations on the free ligands, the π* of MeBtp is at lower energy than π* of Terpy, and interact better with U(5f).

Counterion Effect. To investigate how the nature of the coordination sphere may alter the metal−ligand bond, some calculations were performed on a few complexes where water molecules were replaced by chloride ions. The results, metal−

TABLE 7: Calculated M−N Distances (Å), Contributions of Metal and Ligand to the M−L Bonding Orbitals (%), and Mulliken and Hirshfeld Charges on the Metal Cation in $[M(Terpy)(H_2O)_5Cl]^{2+}$ and $Cm(Terpy)Cl_3$ Clusters

	distances		bonding				charge	
	$M-N_c$	$M-N_d$	description	M (%) d	M (%) s	Terpy (%) total	Mulliken	Hirshfeld
$[Nd(Terpy)(H_2O)_5Cl]^{2+}$	2.59	2.57	σ_1(L→M)	5		91%(σ)		
			σ_2(L→M)	5		92%(σ)	1.64	2.29
			σ_3(L→M)	5		92%(σ)		
$[Am(Terpy)(H_2O)_5Cl]^{2+}$	2.58	2.57	σ_1(L→M)	6	1	92%(σ)		
			σ_2(L→M)	6	1	92%(σ)	1.51	2.34
			σ_3(L→M)	6	1	93%(σ)		
$[Cm(Terpy)(H_2O)_5Cl]^{2+}$	2.56	2.56	σ_1(L→M)	6	1	92%(σ)		
			σ_2(L→M)	6	1	93%(σ)	1.54	2.37
			σ_3(L→M)	5	1	92%(σ)		
$Cm(Terpy)Cl_3$	2.62	2.53	σ_1(L→M)	5	1	92%(σ)		
			σ_2(L→M)	5	1	93%(σ)	1.15	2.26
			σ_3(L→M)	3		95%(σ)		

ligand distances and composition of the M−L bonding, are summarized in Table 7. The complexes correspond to $[M(Terpy)(H_2O)_5Cl]^{2+}$ (M = Nd, Am, Cm) and $[M(Terpy)Cl_3]$. Not surprisingly, as already discussed, metal−nitrogen distances become slightly shorter when a water molecule is replaced by a chloride ion even though the counterion effect on the distance is rather small (≤0.02 Å) for the complexes under consideration.

If the counterion effect on the distance is relatively small, diminishing the total charge of the system could be expected to influence the nature of the bond and in particular to decrease the ligand-to-metal donation and increase the metal-to-ligand donation. However, the calculation shows very similar metal contributions to the bond in $[M(Terpy)(H_2O)_5Cl]^{2+}$ and $[M(Terpy)(H_2O)_6]^{3+}$. Very remarkably, the presence of even three chloride ions in the inner sphere has no significant effect on the curium−ligand bond.

4. Conclusions

The first objective of the study was to test the feasibility and accuracy of quantum chemistry calculations in determining the structural parameters of large actinide(III) and lanthanide(III) complexes with more than 50 atoms. To this end, two theoretical approaches describing relativistic effects have been compared, the molecular model has been tested through the use of a continuum as well as with change of the species present in the coordination sphere, and the results were compared with experimental values when available. A comparison of the structures of lanthanum and curium complexes calculated with small-core RECPs and ZORA reveals no difference between the two theoretical approaches. Presumably because of the strong ionicity of the metal−ligand interaction in the complexes of interest, structural parameters are much more sensitive to the molecular model than to the theoretical approach, and the additional solvent effect beyond the inner coordination sphere, through a continuum model, highlights the significant effect of the molecular model on the structural parameters.

Comparing the calculated and experimental structures shows that the ZORA calculations correctly reproduce the measured bond distances. Agreement between theory and experiment is particularly good when we compare the evolution of the structural parameters as a function of the cation, the choice of the molecular model becoming less critical. Calculations reproduce particularly well the shortening of the uranium−ligand bond/cerium−ligand bond observed experimentally. This is an important result as it is a strong indication of the capability of the DFT/ZORA approach to describe correctly the structures of 4f/5f ions, although the lack of crystal structures for americium(III) and curium(III) complexes prevents complete validation of this theoretical approach.

The other major objective of the study was to probe the nature of the metal−ligand bond. According to the calculations, the lanthanide−ligand distances decrease with the diminishing ionic radius, whereas the actinide−ligand bond increases from uranium to americium and are shorter than Ln−N distances. These trends are explained by the presence of stronger covalent effects in the metal−ligand bond for actinides than lanthanides. However, the increased covalency is significant for uranium but reaches the limit of the calculated approximation for americium and curium. According to this study there is no significant 5f contribution of americium and curium to the bonding. As previously shown for other uranium(III) complexes,[17] the present study confirms the significant participation of the uranium 5f orbital in the metal−ligand bond, with greater mixing for MeBtp ligand than for Terpy, leading to a more significant shortening of the U−N(MeBtp) bond than for U−N(Terpy). These results are coherent with experimental findings that indicate significantly shorter U−N bonds but very small energy differences between the thermodynamic parameters of americium(III), curium(III), and lanthanide(III).

Acknowledgment. The author thank J. C. Berthet at CEA-Saclay for providing unpublished crystal structures of uranium(III) with Terpy. This study was supported by CEA, Direction de la Simulation et des Outils Expérimentaux/Recherche de Base.

References and Notes

(1) *Actinide and Fission Product Partitioning and Transmutation*, OECD/NEA; Proceedings of the Seventh Information Exchange Meeting, Jeju, Republic of Korea, 14−16 October 2002.

(2) Marcus, Y. In *Ion Properties*. Marcel Dekker: New York, 1997.

(3) *Handbook on the Physics and Chemistry of Rare Earths, Vol. 18−Lanthanides/Actinides: Chemistry*; Gschneidner, K. A., Eyring, L., Choppin, G. R., Lander, G. H., Eds.; Elsevier Science: New York, 1994; p 197.

(4) Nash, K. L. *Solvent Extr. Ion Exch.* **1993**, *11*, 729.

(5) Vitorge, P. Complexation de lanthanides et d'actinides trivalents par la TPTZ. Application en extraction liquide-liquide. Ph.D. Thesis, Université Paris 6, France, 1984.

(6) Madic C.; Hudson, M. J.; Liljenzin, J. O.; Nannicini, R.; Glatz, J.-P.; Facchini, A.; Kolarik, Z.; Odoj, R. *Prog. Nucl. Energy* **2002**, *40*, 523.

(7) Boubals, N.; Drew, M. G. B.; Hill, C.; Hudson, M. J.; Iveson, P. B.; Madic, C.; Russell, M. L.; Youngs, T. G. A. *J. Chem. Soc., Dalton Trans.* **2002**, 55.

(8) Cordier, P. Y.; Hill, C.; Baron, P.; Madic, C.; Hudson, M. J.; Liljenzin, J. O. *J. Alloys Compd.* **1998**, *271*, 738.

(9) Kolarik, Z.; Müllich, U.; Gassner, F. *Solvent Extr. Ion Exch.* **1999**, *17*, 23.

(10) Hagstrom, I.; Spjuth, L.; Enarsson, A.; Liljenzin, J. O.; Skalberg, M.; Hudson, M. J.; Iveson, P. B.; Madic, C.; Cordier, P. Y.; Hill, C.; Francois, N. *Solvent Extr. Ion Exch.* **1999**, *17*, 221.

(11) Colette, S.; Amekraz, B.; Madic, C.; Berthon, L.; Cote, G.; Moulin, C. *Inorg. Chem.* **2003**, *42*, 2215.

(12) Colette, S.; Amekraz, B.; Madic, C.; Berthon, L.; Cote, G.; Moulin, C. *Inorg. Chem.* **2002**, *41*, 7031.

(13) Iveson, P. B.; Riviere, C.; Guillaneux, D.; Nierlich, M.; Thuery, P.; Ephritikhine, M.; Madic, C. *Chem. Commun.* **2001**, 1512.
(14) Berthet, J. C.; Riviere, C.; Miquel, Y.; Nierlich, M.; Madic, C.; Ephritikhine, M. *Eur. J. Inorg. Chem.* **2002**, 1439.
(15) Charbonnel, M.-C.; Boubals, N.; Giroux, S.; Guillaumont, D.; Hill, C.; Presson, M.-T.; Roube, C.; Madic, C. Unpublished work.
(16) Miguirditchian, M.; Guillaneux, D.; Guillaumont, D.; Moisy, P.; Madic, C.; Jensen, M.; Nash, K. L. Submitted for publication.
(17) Mazzanti, M.; Wietzke, R. L.; Pecaut, J.; Latour, J. M.; Maldivi, P.; Remy, M. *Inorg. Chem.* **2002**, *41*, 2389.
(18) van Lenthe, E.; Ehlers, A.; Baerends, E. J. *J. Chem. Phys.* **1999**, *110*, 8943.
(19) van Lenthe, E.; Baerends, E. J.; Snijders, J. G. *J. Chem. Phys.* **1993**, *99*, 4597.
(20) van Lenthe, E.; Baerends, E. J.; Snijders, J. G. *J. Chem. Phys.* **1994**, *101*, 9783.
(21) Dolg, M.; Stoll, H.; Savin, A.; Preuss, H. *Theor. Chim. Acta* **1989**, *75*, 173.
(22) Küchle, W.; Dolg, M.; Stoll, H.; Preuss, H. *J. Chem. Phys.* **1994**, *100*, 7535.
(23) Wang, D. Q.; Zhao, C. Y.; Phillips, D. L. *Organometallics* **2004**, *23*, 1953.
(24) Vazquez, J.; Bo, C.; Poblet, J. M.; de Pablo, J.; Bruno, J. *Inorg. Chem.* **2003**, *42*, 6136.
(25) Hay, P. J. *Faraday Discuss.* **2003**, *124*, 69.
(26) Joubert, L.; Maldivi, P. *J. Phys. Chem. A* **2001**, *105*, 9068.
(27) Bolvin, H.; Wahlgren, U.; Moll, H.; Reich, T.; Geipel, G.; Fanghanel, T.; Grenthe, I. *J. Phys. Chem. A* **2001**, *105*, 11441.
(28) Hay, P. J.; Martin, R. L. *J. Chem. Phys.* **1998**, *109*, 3875.
(29) Maron, L.; Eisenstein, O. *J. Phys. Chem. A* **2000**, *104*, 7140.
(30) te Velde, G.; Bickelhaupt, F. M.; van Gisbergen, S. A. J.; Fonseca Guerra, C.; Baerends, E. J.; Snijders, J. G.; Ziegler, T. *J. Comput. Chem.* **2001**, 931.
(31) Fonseca Guerra, C.; Snijders, J. G.; te Velde, G.; Baerends, E. J. *Theor. Chem. Acc.* **1998**, 391.
(32) ADF2002.03, SCM, Theoretical Chemistry, Vrije Universiteit, Amsterdam, The Netherlands; http://www.scm.com.
(33) Becke, A. D. *Phys. Rev. A* **1988**, *38*, 3098.
(34) Perdew, J. P. *Phys. Rev. B* **1986**, *33*, 8822.
(35) Frisch, M. J.; Trucks, G. W.; Schlegel, H. B.; Scuseria, G. E.; Robb, M. A.; Cheeseman, J. R.; Zakrzewski, V. G.; Montgomery, J. A.; Stratmann, R. E.; Burant, J. C.; Dapprich, S.; Millam, J. M.; Daniels, A. D.; Kudin, K. N.; Strain, M. C.; Farkas, O.; Tomasi, J.; Barone, V.; Cossi, M.; Cammi, R.; Mennucci, B.; Pomelli, C.; Adamo, C.; Clifford, S.; Ochterski, J.; Petersson, G. A.; Ayala, P. Y.; Cui, Q.; Morokuma, K.; Malick, D. K.; Rabuck, A. D.; Raghavachari, K.; Foresman, J. B.; Cioslowski, J.; Ortiz, J. V.; Baboul, A. G.; Stefanov, B. B.; Liu, G.; Liashenko, A.; Piskorz, P.; Komaromi, I.; Gomperts, R.; Martin, R. L.; Fox, D. J.; Keith, T.; Al-Laham, M. A.; Peng, C. Y.; Nanayakkara, A.; Gonzalez, C.; Challacombe, M.; Gill, P. M. W.; Johnson, B.; Chen, W.; Wong, M. W.; Andres, J. L.; Gonzalez, C.; Head-Gordon, M.; Replogle, E. S.; Pople, J. A. *Gaussian 98*, Revision A.9; Gaussian, Inc.: Pittsburgh, PA. 1998.
(36) Becke, A. D. *J. Chem. Phys.* **1993**, *98*, 5648.
(37) Stephens, P. J.; Devlin, F. J.; Chabalowski, C. F.; Frisch, M. J. *J. Phys. Chem.* **1994**, *98*, 11623.
(38) Barone, V.; Cossi, M. *J. Phys. Chem. A* **1998**, *102*, 1995.
(39) Cosentino, U.; Villa, A.; Pitea, D. *J. Phys. Chem. B* **2000**, *104*, 8001.
(40) Vetere, V.; Maldivi, P.; Adamo, C. *J. Comput. Chem.* **2003**, *24*, 850.
(41) Allen, F. H. *Acta Crystallogr.* **2002**, *B58*, 380.
(42) Bruno, I. J.; Cole, J. C.; Edgington, P. R.; Kessler, M.; Macrae, C. F.; McCabe, P.; Pearson, J.; Taylor, R. *Acta Crystallogr.* **2002**, *B58*, 389.
(43) Kepert, C. J.; Weimin, L.; Skelton, B. W.; White, A. H. *Aust. J. Chem.* **1994**, *47*, 365.
(44) Conradson, S. D. *Appl. Spectrosc.* **1998**, *52*, 252A.
(45) Allen, P. G.; Bucher, J. J.; Skuh, D. K.; Edelstein, N. M.; Craig, I. *Inorg. Chem.* **2000**, *39*, 595.
(46) Matonic, J. H.; Scott, B. L.; Neu, M. P. *Inorg. Chem.* **2001**, *40*, 2638.
(47) Blaudeau, J.-P.; Zygmunt, S. A.; Curtiss, L. A. *Chem. Phys. Lett.* **1999**, 347.
(48) Pavlov, M.; Siegbahn, P. E. M.; Sandstrom, M. *J. Phys. Chem. A* **1998**, *102*, 219.
(49) Martinez, J. M.; Pappalardo, R. R.; Marcos, E. S. *J. Phys. Chem. A* **1997**, *101*, 4444.
(50) Martinez, J. M.; Pappalardo, R. R.; Marcos, E. S.; Mennucci, B.; Tomasi, J. *J. Phys. Chem. B* **2002**, *106*, 1118.
(51) Shannon, R. D. *Acta Crystallogr.* **1976**, *A32*, 751.
(52) David, F. *J. Less Common Met.* **1986**, *121*, 27.
(53) David, F. H.; Fourest, B. *New J. Chem.* **1997**, *21*, 167.
(54) Hirshfeld, F. L. *Theor. Chim. Acta* **1977**, *44*, 129.
(55) Semenova, L. I.; White, A. H. *Aust. J. Chem.* **1999**, *52*, 539.
(56) Berthet, J. C.; Miquel, Y.; Iveson, P. B.; Nierlich, M.; Thuéry, P.; Madic, C.; Ephritikhine, M. *J. Chem. Soc., Dalton Trans.* **2002**, 3265.